minerals

MDPI

Article

Influence of pH and Contaminant Redox Form on the Competitive Removal of Arsenic and Antimony from Aqueous Media by Coagulation

Muhammad Ali Inam [1], Rizwan Khan [1], Du Ri Park [1], Babar Aijaz Ali [2], Ahmed Uddin [3] and Ick Tae Yeom [1,*]

1 Graduate School of Water Resources, Sungkyunkwan University (SKKU) 2066, Suwon 16419, Korea; aliinam@skku.edu (M.A.I.); rizwankhan@skku.edu (R.K.); enfl8709@skku.edu (D.R.P.)
2 College of Environmental Science and Engineering, Donghua University, Shanghai 201620, China; babaraijaz40@hotmail.com
3 Key Laboratory of Jiangsu Province for Chemical Pollution Control and Resources Reuse, School of Environmental and Biological Engineering, Nanjing University of Science and Technology, Nanjing 210094, China; jamali@njust.edu.cn
* Correspondence: yeom@skku.edu; Tel.: +82-31-299-6699

Received: 24 October 2018; Accepted: 3 December 2018; Published: 6 December 2018

Abstract: In most countries, arsenic (As) and antimony (Sb) are regulated pollutants, due to their significant impacts on the environment and human health. Iron-based (Fe) coagulants play a fundamental role in the removal of both elements from aqueous media. This study aims to investigate the competitive removal of As and Sb in relation to Fe solubility. Coagulation experiments were conducted in synthetic water under various pH and contaminant loading, using ferric chloride (FC) as a coagulant. In the single system, the pentavalent species significantly reduced the Fe solubility and thereby enhanced the mobility of As and Sb under these environmental conditions. The coexistence of pentavalent and trivalent species in the binary system considerably decreases the Fe solubility at acidic conditions while enhancing the dissolution under alkaline conditions, thus affecting the overall removal of both species. The presence of four redox species in the quaternary system decreases the Fe solubility remarkably over a wide pH range, with better Sb removal, as compared to As under similar conditions. The adsorption study of the single system showed a decrease in As(V) adsorption capacity at higher concentration, while in the binary system, the Sb(III) showed strong adsorption potential, compared to other species. In the quaternary system, the presence of all four redox species has a synergistic effect on total Sb adsorption, in comparison to the total As. Furthermore, the results of Fourier transform infrared (FT-IR) analysis of FC composite contaminant flocs confirm that the combined effect of charge neutralization and inner sphere complexation might be a possible removal mechanism. These findings may facilitate the fate, transport and comparative removal of redox species in the heterogeneous aquatic environment.

Keywords: arsenic; antimony; coagulation; competitive removal; ferric chloride; water treatment

1. Introduction

Arsenic (As) and antimony (Sb) have numerous applications, including the manufacture of plastics, batteries, flame retardants and semiconductor materials [1–3]. A recent research survey [4] indicated that the global annual consumption of Sb was 188,000 tons, about fivefold more than that of As. As a result, anthropogenic emission causes As and Sb concentrations in soils and waters that greatly exceed their baseline concentrations [5]. It is estimated that a large population of Bangladesh and West Bengal has been affected, due to the consumption of As-contaminated groundwater [6].

The high levels of co-occurring As and Sb in soils and waters are mostly found in the vicinity of mining and smelting areas [7,8]. Moreover, the groundwater near abandoned Sb mines in Slovakia presented high Sb levels of up to 1 mg/L [9]. A recent study [10,11] reported the concentration of Sb (6 mg/L) in underground well water and high contamination of Sb (5045 mg/Kg) and As (205 mg/Kg) in the soils near Xikuangshan Sb mine, China. Therefore, the release of these toxic elements from different sources into the environment has raised global concerns regarding their potential risk of exposure to human, as well as the aquatic environment.

The oxidation state of As and Sb in soil and aquatic environment strongly depend upon the system redox and pH. They are both mostly found in inorganic forms, that is, trivalent (As(III) and Sb(III)) under naturally reducing environment and pentavalent (As(V) and Sb(V)) species under toxic surroundings [12]. The trivalent species predominantly exist as $As(OH)_3$ and $Sb(OH)_3$ under the most natural water pH conditions [13,14]. Furthermore, the inorganic As(V) species occur in the forms of $H_2AsO_4^-$, $HAsO_4^{2-}$ at pH (2.20–9.22) and Sb(V) is in the deprotonated form of antimonic acid as $Sb(OH)_6^-$ at pH > 2.72 [15,16]. Previous studies [17] indicated that the trivalent form of both elements is tenfold more toxic in comparison with the pentavalent species. For example, the consumption of As-polluted water can cause severe health effects, such as lung and bladder cancers, as well as various kinds of skin lesions [18]. In addition, the adverse health effects of the oral uptake of water-soluble Sb in the human body, such as abdominal cramps, cardiac toxicity, vomiting and diarrhea, have also been well reported [19]. Therefore, due to the toxicological effect on human health, both elements are listed as pollutants of priority interest by the Council of European Union (EU) and the United States Environmental Protection Agency (USEPA) [17]. Furthermore, the Ministry of Environment in South Korea has recently included Sb in the monitoring list of the Water Quality and Aquatic Ecosystem Conservation Act planned to come into effect in January 2019 [20]. The USEPA has set high regulation standards of 10 μg/L As and 5 μg/L Sb for drinking water, to minimize the harmful effects of both elements on human health. Moreover, the World Health Organization (WHO) also established 10 μg/L as the guideline value for both elements in drinking water [17]. Therefore, it is necessary to remove both contaminants from drinking water sources, to reduce the possible associated risks.

Iron (Fe) minerals are considered important scavengers for As and Sb, due to their widespread distribution, large surface area and strong adsorption capability for heavy metals [21,22]. Fe-based coagulants, such as ferric chloride (FC), can regulate the concentration of soluble As and Sb species in surface/subsurface waters[23]. While the precipitation of Fe is the major pathway of Fe oxides, the dissolution of co-precipitated Fe may occur via reductive or non-reductive means in the heterogeneous aqueous environment [24]. The reductive dissolution of Fe may either be accomplished with various natural organic matter (NOM), protons, complex-forming ligands, or inorganic reductants (e.g., HS^-, Fe^{2+}, OH^-) [24,25]. The inorganic reductants may notably influence the Fe solubility by changing physicochemical environments, such as pH, Fe^{2+} concentrations, phase transformation, inner spherical electron transfer and surface complexation reactions [26]. A recent study [27] has reported that NOM might enhance Fe(III) oxide dissolution, due to the formation of surface complexes. In our earlier study [13], the dissolution of Fe(III) precipitates in the presence of inorganic ligand like $Sb(OH)_6^-$ under alkaline conditions was intensively investigated. The complete dissolution of Fe(III) precipitates was observed due to the complexation of Fe with $Sb(OH)_6^-$ and strong electron transfer from $Sb(OH)_6^-$ to Fe(III), resulting in the breaking of Fe–O bond in the mineral lattice [13]. In other words, this significantly influences the Fe(III) stability, thereby affecting the fate and mobility, as well as the removal behavior, of pollutants in natural waters [28,29]. Therefore, the geochemical and competitive removal behavior of coexisting As and Sb under heterogeneous aqueous environment is worth understanding.

Many researchers [30–32] have investigated the simultaneous removal performance of As and Sb in the multicomponent environment. The factors, such as pH, coagulant type and dosage, initial contaminant levels and NOM, affect the As or Sb adsorption onto the surface of Fe minerals [33,34]. A result of a recent study [35] on simultaneous adsorption by ferrihydrite reported the synergistic effect

on Sb(III) removal, while the antagonistic effect on Sb(V) removal, over a wide pH range. Moreover, Sb(III) demonstrated strong adsorption potential irrespective of pH in the presence of coexisting As and Sb species [36]. Our previous study [13] has shown the significant inhibition of Sb removal under coexisting Sb(III, V) conditions with higher Sb(V) fraction using FC coagulation. The higher adsorption capacity of poorly crystalline coagulant has been also reported [34]. Some recent studies [1,36,37] have shown the variable coagulation efficiencies of As and Sb in a binary system. The promotional effect on As(V) adsorption by ferrihydrite was observed in the presence of Sb(V) media [1]. Moreover, the strong inhibition of As(III) adsorption in the presence of Sb(III) in their binary system has been reported [36]. In contrast, some researchers [37] have shown that both As and Sb adsorption rates will be enhanced as compared to a single solute system and high removal of these contaminants can be achieved by potassium ferrate in the binary system. However, studies reported in the literature are limited to the competitive adsorption behavior of As and Sb on various Fe minerals. In addition, a number of studies [38–42] had been conducted using FC coagulant for As or Sb removal from water but all these studies were limited to removal of single contaminant that is, either As or Sb species. To the best of our knowledge, no study has been conducted so far which provide the knowledge on simultaneous removal behavior of coexisting As and Sb species from water using FC as a coagulant. The previous literature also seems insufficient regarding the competitive As–Sb removal in relation to Fe solubility using FC coagulation in the heterogeneous aqueous environment.

The aim of this study is therefore to investigate the effect of As and Sb on Fe solubility in the single, binary and quaternary system at various pH, as well as different contaminant loading. This work also aims to evaluate the As and Sb removal under similar environmental conditions, to better understand the fate, mobility and transport of these contaminants in aqueous media. The yielded data were further used to clarify the removal mechanism of both elements in a complex environment.

2. Materials and Methods

2.1. Materials and Solutions Preparation

All the chemicals used in this study were of analytical reagent grade. The antimony (III) oxide (Sb_2O_3), arsenic (III) oxide (As_2O_3), potassium hexahydro-antimonate ($KSb(OH)_6$) and sodium arsenate dibasic heptahydrate ($Na_2HAsO_4{\cdot}7H_2O$) were purchased from Sigma Aldrich (St. Louis, MO, USA); while iron (III) chloride hexahydrate ($FeCl_3{\cdot}6H_2O$), nitric acid (HNO_3), hydrochloric acid (HCl) and sodium hydroxide were obtained from the local suppliers. The stock solutions (100 mg/L) of Sb(III) and As(III) were prepared by dissolving Sb_2O_3 and As_2O_3 in 2 M HCl and 1 M NaOH solutions, respectively. The remaining stock solutions (100 mg/L) of Sb(V) and As(V) and 0.1 M Fe(III) were prepared by dissolving $KSb(OH)_6$, $Na_2HAsO_4{\cdot}7H_2O$ and $FeCl_3{\cdot}6H_2O$ in deionized (DI) water. Prior to use, all glassware and polyethylene bottles were washed with 15% HNO_3 solution and then rinsed with DI water.

2.2. Coagulation Experiments

2.2.1. Experimental Conditions

The coagulation experiments were conducted to study the effect of pH (4–10) on Fe solubility and As, Sb removal, where 0.1 mM (27.029 mg/L) FC dose was used for solutions with 1 mg/L As(III, V) and Sb(III, V), respectively [13]. The experiments were also performed to study the competitive interactions of either As and Sb species in various binary systems over a broad pH range, where solutions contain single As and Sb species. The concentration of each species in a binary system was maintained at 1 mg/L. Following this procedure, additional experiments were conducted for the quaternary system over a wide pH range. The referred pH range (4–10) was selected since it provides information on As and Sb removal behavior at acidic (4–6), neutral (7) and basic (8–10) pH conditions. The follow-up experiments were performed under neutral pH conditions. The adsorption isotherm

experiments were conducted in a single system by varying the initial As and Sb concentrations from (0.1–10) mg/L. The competitive adsorption isotherm experiments of As(III, V) and Sb(III, V) were also performed to investigate the adsorption affinity under binary and quaternary system over various initial concentrations of (0.1–10) mg/L for each species. All experiments were conducted at room temperature (RT).

2.2.2. Jar Test Procedure

Prior to coagulation experiment, the 100 mL of working solution was transferred to a 250 mL beaker. The optimum FC dose, that is, 0.1 mM was set for all experiments [13,33] and pH was adjusted using 0.1 M HCl and 0.1 M NaOH solution. Before the measurement of pH, the pH meter was calibrated with buffer solutions of (4.01, 7.00 and 10.01) at 25 °C. The coagulation experiments were conducted using a jar tester equipment (Model: SJ-10, Young Hana Tech Co., Ltd., Gyeongsangbuk-Do, Korea). The coagulation procedure followed the same method as described in our previous study [13] and briefly described as (1) rapid mixing at 140 rpm for 3 min; (2) slow mixing at 40 rpm for 20 min; and (3) settling for 30 min. The aliquot was then filtered using 0.45 μm glass fiber filter, collected and analyzed for the residual concentration of each species. The adsorption density (q_e, g/mol) of As and Sb towards precipitated Fe was calculated using Equation (1):

$$q_e = \frac{C_o - C_e}{C_{Fe}} \quad (1)$$

where, C_o (mg/L) is the initial and C_e (mg/L) is the aliquot concentration of As and Sb and C_{Fe} (mM) is the concentration of Fe precipitates in the solution.

2.2.3. Adsorption Isotherm Models

To further elucidate the adsorption affinity of each As and Sb species under neutral pH, experimental data and goodness of fit of selected isotherms (Langmuir and Freundlich models) were acquired at different contamination levels. Moreover, these isotherm models are commonly used to study various adsorption process under the single and coexisting system. Langmuir isotherm assumes that homogeneous adsorption on the adsorbent surface sites with the same energy, while the Freundlich model assumes that adsorption takes place on the specific heterogeneous sites of the adsorbent [43,44]. The nonlinear forms of the Langmuir and Freundlich isotherms are given by Equations (2) and (3), respectively:

$$q_e = \frac{q_m K_L C_e}{1 + K_L C_e} \quad (2)$$

$$q_e = K_F C_e^{\frac{1}{n}} \quad (3)$$

where q_e (g/mol) is the amount of As and Sb species adsorbed on FC surface sites; C_e (mg/L) is the equilibrium concentration of As and Sb in solution; q_m and K_L in Langmuir equation represent the maximum adsorption affinity and Langmuir constant related to adsorption energy; K_F and n in Freundlich equation represent the constant related to the adsorption capacity and intensity of heterogeneity, respectively.

2.3. Other Analytical Methods

The residual concentration was analyzed by Inductively Coupled Plasma Optical Emission Spectrometry (ICP-OES: Model Varian, Agilent technologies, Sana Clara, CA, USA). The precise detection limits of ICP-OES for Fe, As and Sb are 0.001, 0.007 and 0.003 mg/L respectively while, the quantification limits are 0.0035, 0.048 and 0.01 mg/L for Fe, As and Sb respectively. The pH of the solution was measured by pH meter (HACH: HQ40d Portable pH, Conductivity, oxidation-reduction potential (ORP) and ion selective electrode (ISE) Multi-Parameter Meter, Hach Company, Loveland, CO, USA). The Fourier Transform Infrared Spectroscopy (FT/IR-4700, spectroscopy and JASCO Analytical

Instruments, Easton, PA, USA) results of the precipitated Fe after interaction with As-Sb in the range (400–4000) cm^{-1} were used to investigate the bonding features. The speciations of As, Fe and Sb were obtained using Visual MINTEQ 3.1 (KTH, Stockholm, Sweden).

3. Results and Discussion

3.1. Effect of pH on Fe Solubility and As and Sb Removal by Coagulation

The speciations of As, Fe and Sb as a function of pH were derived to better understand the influence of pH on these species during the removal process, as shown in (Supplementary Information (SI): Figure S1 and Table S1). It can be observed that the dominant form of Fe(III) over the pH range (3.76–8.48) is $Fe(OH)_2^+$, while at pH above 8.48, $Fe(OH)_4^-$ occurs (Figure S1). Moreover, the small fraction of $Fe(OH)_3$ in the pH range (7.67–9.27) can also be observed. The As and Sb speciations in an aqueous environment are mainly controlled by the redox conditions and pH of the solution [17]. Table S1 shows that when pH ranges below (9.22 to 10.4), the trivalent forms, that is, arsenite (As(III)) and antimonite (Sb(III), exist in the form of H_3AsO_3 and $Sb(OH)_3$, respectively. Similarly, in the pH range (2.7–11.53), the pentavalent forms, that is, arsenate (As(V)) and antimonate (Sb(V)), can be either $H_2AsO_4^-$ or $HAsO_4^{2-}$ and $Sb(OH)_6^-$, respectively. In general, the inorganic forms of As and Sb in natural waters, which are typically in the pH range (4–8), include trivalent forms of H_3AsO_3 and $Sb(OH)_3$ and pentavalent forms of $H_2AsO_4^-$ or $HAsO_4^{2-}$ and $Sb(OH)_6^-$, respectively.

3.1.1. Single Solute System

Figure 1A shows the Fe solubility behavior as a function of pH using FC coagulation in a single solute system. The dotted line of "Control" indicates the Fe solubility in the absence of As and Sb species, while the four solid lines represent the Fe solubility in the presence of both species. At "Control" conditions, the Fe solubility gradually decreases from 65.4%–49.4% (pH (4 to 5)) and FC precipitates become insoluble upon further increase of pH from (6–10). The presence of Sb(III, V) species showed the negligible effect on Fe solubility under extremely acidic conditions, that is, pH (4–5). In contrast, the presence of As(III, V) species showed a remarkable decrease in Fe solubility at those conditions. Such observation could be explained by the solution complexes and destabilization of Fe(III) by As species under the highly acidic conditions [14]. For example, the intrinsic surface complexation constant log K for As(V)/$Fe(OH)_3$ complex of 25.83 was about three times greater than that of Sb(V)/$Fe(OH)_3$ complex of 8.4 [34,45]. It is likely that the adsorbed As(V) on precipitated Fe may also facilitate the Fe coagulation and flocculation process. Therefore, the Fe solubility is significantly reduced, due to the stronger affinity between As(V) and $Fe(OH)_3$. Moreover, in the case of As(V), the increase in the supernatant pH from (5 to 5.57) was observed (Table S2 of the Supplementary Information (SI)). Thus, the closeness of pH near/at the isoelectric point (IEP) of FC may also be responsible for the significant decrease in Fe solubility in the presence of As(V), as compared to Sb(V) [14]. However, the Fe solubility was found negligible under neutral pH conditions in the absence and presence of As and Sb species. The Fe solubility under extreme basic conditions was enhanced to 84%–100% in the presence of As(V) and Sb(V) species. These results are consistent with previous studies that suggested the increase in Fe(III) solubility due to the effect of ligand-induced dissolution [13,14].

Moreover, the release of Fe(III) into the solution might be enhanced due to the inner sphere complexation of anionic ligands molecules with surface groups of Fe [46–49]. The surface charge of ligands may also be responsible for the increase in Fe solubility under these conditions. As discussed above, the dominant form of As(V)/Sb(V) was $HAsO_4^{2-}$/$Sb(OH)_6^-$ (Table S1), while the Fe(III) existed as $Fe(OH)_4^-$ under extremely basic conditions (Figure S1). The As(V)/Sb(V) species may act as an inorganic ligand binding to Fe(III) hydroxyl complex. Two modes of Fe(III) release in response to ligand sorption can be proposed, considering the association of Fe(III) on As(V)/Sb(V) [39]. First, either the attachment of As(V) or Sb(V) occurs through chemical bond (≡Fe–O–As≡ or ≡Fe–O–Sb≡) at the $Fe(OH)_3$ interface, resulting in the formation of surface active species (≡$FeAsO_4^{2-}$

or ≡FeOSbO$(OH)_4^-$), thus weakening the Fe–O bond and leading to detachment of the Fe–As or Fe–Sb groups [34,39,45]. The bond breaking at the interface of $Fe(OH)_3$ would lead to the release of Fe(III) in solution, thereby enhancing Fe solubility. Secondly, the attachment of As(V) or Sb(V) through $Fe(OH)_3$ surface interaction energy would lead to the release of Fe complex [39]. The stability of Fe(III) lattice may be affected by the van der Wall (vdW) forces of attraction and electrostatic repulsive forces, as described by the Derja-Guin-Landau-Verwey-Overbeek (DLVO) theory [50]. Initially, the precipitated Fe is held to the Fe(III) surface by dominant vdW attractive forces. The introduction of anionic ligands (As(V) or Sb(V)) will result in its adsorption on the precipitated Fe. This ultimately brings higher negative charge density on the $Fe(OH)_3$ surface, which in turn increase the electrostatic repulsive forces between the molecules [51]. A negligible amount of energy is required to detach the Fe–As or Fe–Sb complex from the surface lattice. Thus the lowering of energy barrier as a result of interaction under these conditions may significantly enhance the dissolution of Fe atoms [51]. The Fe solubility was therefore remarkably increased in the presence of As(V) or Sb(V) species under extreme basic conditions.

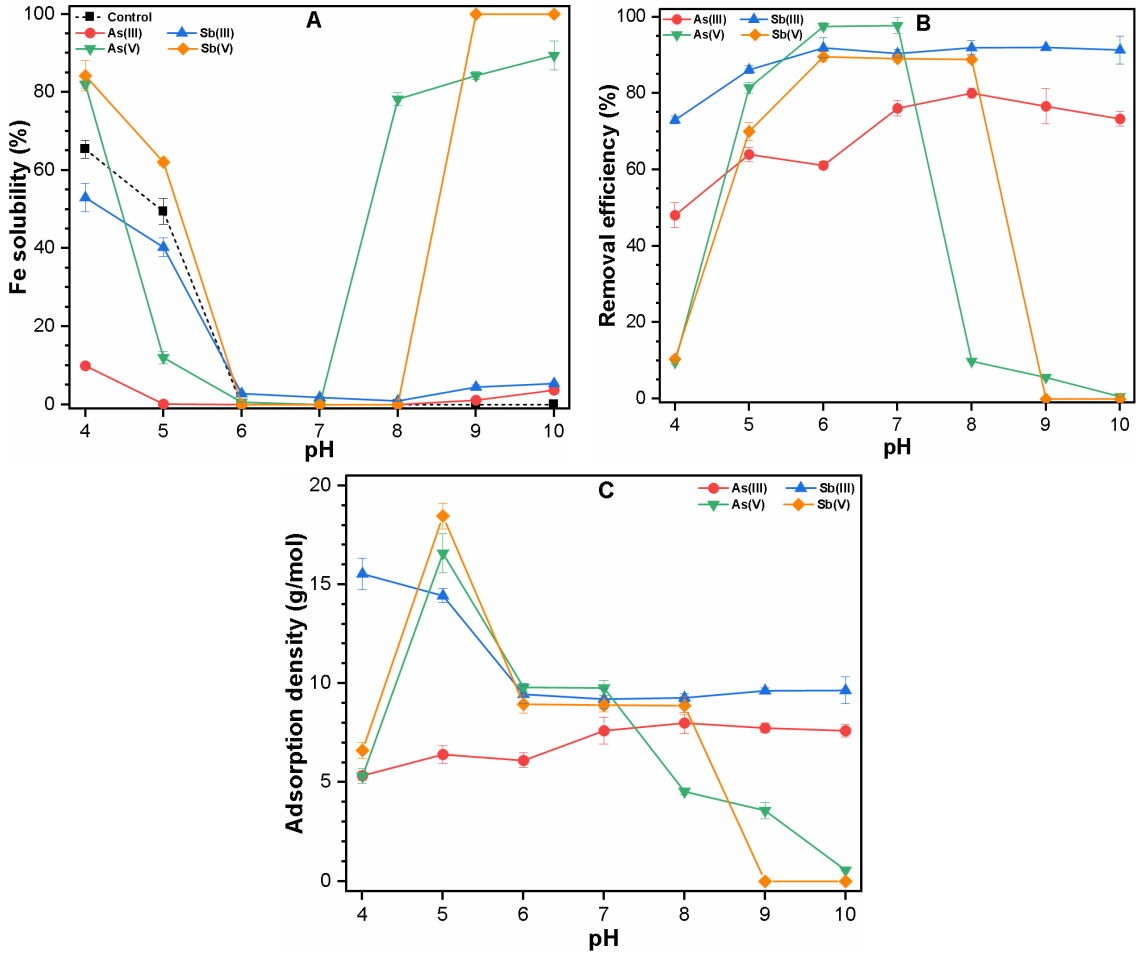

Figure 1. Single solute system of As and Sb species showing (**A**) Fe solubility (%); (**B**) removal efficiency (%); (**C**) adsorption densities (g/mol) under various pH in the range (4–10) with 0.1 mM FC coagulant dose.

Figure 1B presents the removal of As and Sb species by FC coagulation over various pH ranging (4–10). Interestingly, the removal behavior of these species was in close relation to the Fe solubility. The removal of As(III) and Sb(III) was enhanced upon increasing pH, due to the decrease in Fe solubility (Figure 1A,B). These results are consistent with the previous findings [13,14]. The Sb(III) removal was found relatively higher than the As(III) (Figure 1B), which may be ascribed to Sb(III) being

a stronger Lewis base than As(III) [15]. Moreover, the first dissociation constant pKa of $Sb(OH)_3$ (10.4) was also higher than the H_3AsO_3 (9.22), as shown in Table S1. Under such pH edge, Fe(III) existed as $Fe(OH)_2^+$ between pH (3.76 and 8.48) and $Fe(OH)_4^-$ above pH 8.48 (Figure S1); thus $Sb(OH)_3$ might strongly diffuse into the Fe precipitate surface, regardless of the charge potential required to engage in the adsorption process [13]. Furthermore, considering the surface sites of amphoteric precipitated Fe as Lewis acids, the interaction of Sb(III) and the Fe precipitate surface sites would be much higher than As(III) [36]. To further evaluate the adsorption strength of As(III) and Sb(III), the adsorption density of both species were calculated and also presented in Figure 1C. Similar to the removal behavior, higher adsorption potential of Sb(III) was obtained as compared to As(III) over the entire pH range.

In contrast, the removal behaviors of As(V) and Sb(V) were more strongly affected by pH (Figure 1B), due to the significant change of Fe solubility with pH (Figure 1A). Unsurprisingly, As(V) and Sb(V) were preferentially removed at acidic conditions and showed the highest removal at pH (6 and 7), owing to the sufficient availability of FC precipitates (Figure 1A,B). However, the removal efficiency of both species decreased significantly at pH (9 and 10), due to the increase in Fe solubility (>90%) (Figure 1A,B). The adsorption potentials of As(V) and Sb(V) were found highest at pH 5 (16.57 g/mol As(V), 18.46 g/mol Sb(V)), at pH (6–7) (~9.80 g/mol As(V), Sb(V)) with decreasing trend upon further increasing pH (Figure 2C). It can be observed that when the pH ranges (4–10), the arsenate and antimonate exist as anionic forms of $H_2AsO_4^-$ (pKa: 2.2), $HAsO_4^{2-}$ (pKa: 6.97) and $Sb(OH)_6^-$ (pKa: 2.7), respectively (Table S1). These results suggest that the electrostatic attraction of these negatively charged As(V) or Sb(V) and positively charged Fe(III) hydroxyl species favors the highest As(V) or Sb(V) diffusion, as well as adsorption on the FC precipitates at the acidic pH conditions [14,33,45]. However, at basic pH conditions, both contaminants and FC precipitates were negatively charged, resulting in higher Fe solubility (Figure 1A) and hinder the As(V) or Sb(V) diffusion and adsorption process, due to the strong electrostatic repulsion. In addition, the competition of OH^- with As(V) or Sb(V) on FC precipitate surface might also contribute towards the poor adsorption of these species specifically at higher pH values [33,45]. In summary, the adsorption sequence of As and Sb over a wide pH range can be elucidated in a single solute system. The adsorption potential of As and Sb species during FC coagulation in a single system at pH (5, 7 and 9) can be arranged in the orders of (Sb(V) > As(V) > Sb(III) > As(III)), (As(V) > Sb(III) > Sb(V) > As(III)) and (Sb(III) > As(III) > As(V) > Sb(V)), respectively.

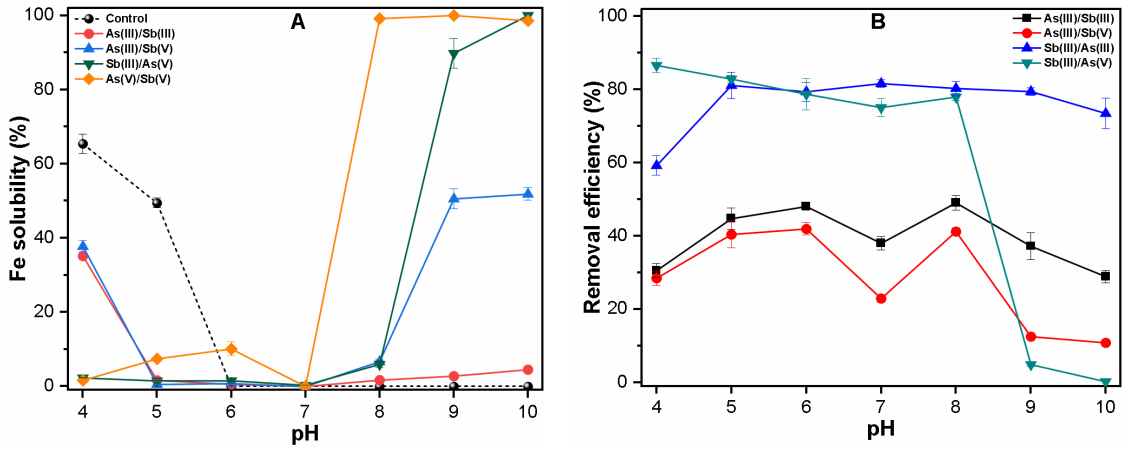

Figure 2. *Cont.*

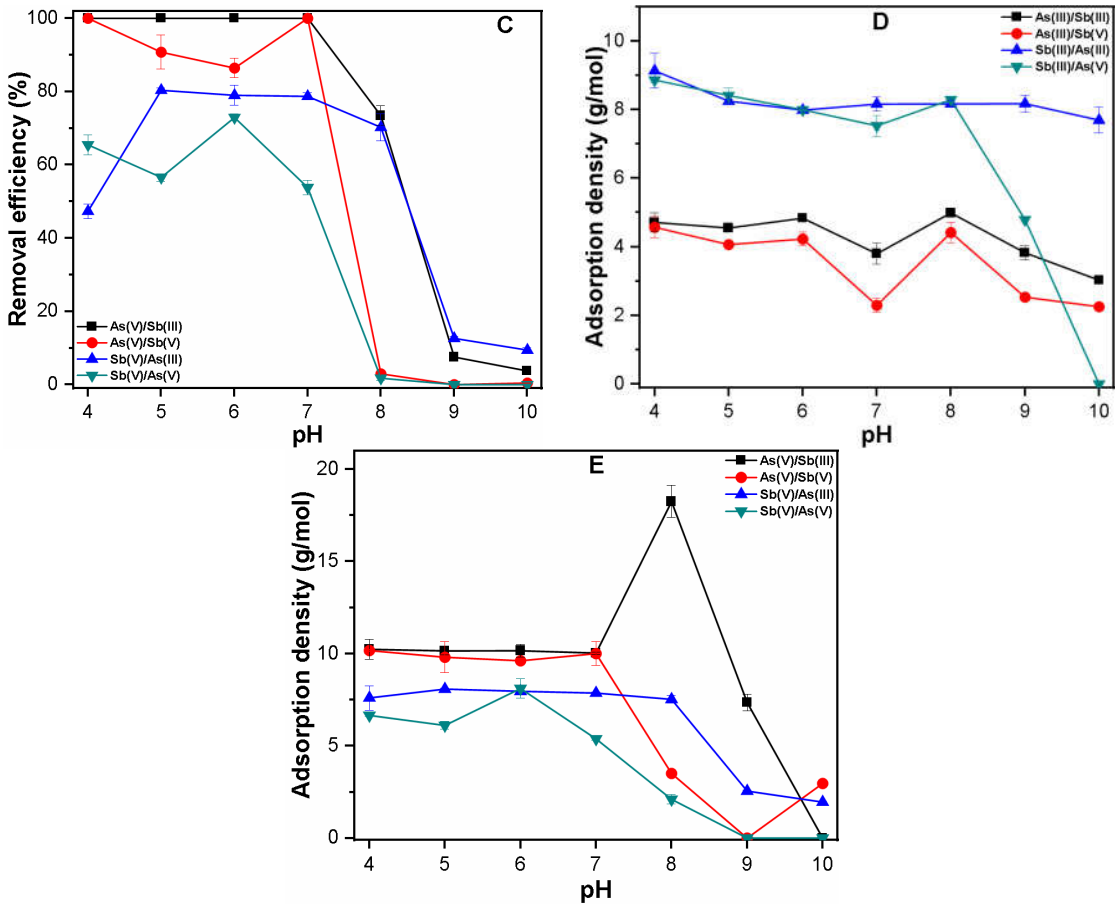

Figure 2. Binary system of As and Sb species showing (**A**) Fe solubility (%); (**B**,**C**) Removal efficiency (%); (**D**,**E**) Adsorption densities (g/mol) under various pH range (4–10) with 0.1 mM FC coagulant dose.

3.1.2. Binary System

Figure 2A shows the Fe solubility as a function of pH using FC in the binary systems of As(III)/Sb(III), As(III)/Sb(V), Sb(III)/As(V) and As(V)/Sb(V). It is worth noting that in all binary systems, the Fe solubility was significantly reduced at acidic pH; however, negligible effect on Fe solubility was observed under neutral pH. This observation may be attributable to the presence of As species imparting a great effect on Fe solubility under acidic pH range, as already observed in a single system (Figure 1A), thereby allowing more Fe precipitation. The change in pH was also monitored under all binary systems, which showed its negligible role in the change in Fe solubility (Table S3 of the SI). Moreover, the Fe(III) hydroxyl complex existed as $Fe(OH)_2^+$, the As(III) and Sb(III) species occurred as H_3AsO_3 and $Sb(OH)_3$ respectively, while the As(V) and Sb(V) species existed as $HAsO_4^-$ and $Sb(OH)_6^-$ under acidic pH range (4–5) (Figure S1 and Table S1). It can be assumed that under acidic conditions, the positively charged Fe(III) hydrolyzed species would attract the negatively charged dissociated As(V) and Sb(V) species, thereby decreasing the stability and neutralizing the overall surface charge of Fe(III)-complexes in the system.

The existence of As(III) and Sb(III) species in such environment will cause interaction with these species on the surface sites of Fe(III)-complex, as well as dissociated Fe(III) hydrolyzed species; thus drastically decreasing the Fe solubility under acidic conditions [52]. Moreover, the FC precipitates become completely insoluble in the As(V)/Sb(V) binary system under acidic conditions (Figure 2A). This might be attributed to the more negative surface charge of these species at an acidic condition, which promotes strong attraction towards positively charged dissociated Fe(III) hydrolyzed species, as shown in Table S1. On the other hand, the Fe solubility was enhanced in the binary system of As(V)/Sb(V) under alkaline conditions (viz. pH (9–10)). The effect of As(V) on Fe solubility as

compared to Sb(V) was more pronounced at the basic environment, thus promoting Fe dissolution around 90%–100% in binary systems of Sb(III)/As(V) and As(V)/Sb(V) under these conditions (Figure 2A). This may be attributable to the much stronger electron donation from $HAsO_4^{2-}$ to $Fe(OH)_4^-$ than $Sb(OH)_6^-$ easily eliminating the electron density between Fe and oxygen atoms of the mineral lattice [51]. This results in the weakening of the Fe–O bond and lowering the energy barrier among molecules, which promotes the Fe dissolution in the binary system [51]. Similarly, the presence of Sb(V) in the As(III)/Sb(V) binary system enhanced the Fe solubility (50%) under alkaline conditions. In contrast, the As(III)/Sb(III) binary system indicated the negligible effect on Fe solubility under basic environment, as presented in Figure 2A.

To understand the effect of pH on competitive As and Sb removal by FC coagulation, experiments were performed with As and Sb binary systems over a broad pH range (4–10) (Figure 2B–E). The presence of Sb(III) and Sb(V) species indicated the inhibitory effect on As(III) removal over a broad pH range (Figure 2B). The more prominent adverse effect on As(III) removal was observed under the influence of Sb(V), specifically at alkaline pH. This may be ascribed to either the competition of As(III) and Sb(V) on surface sites, or lesser available FC precipitates might result in significant inhibition of As(III) removal under these conditions (Figure 2A,B). Therefore, the adsorption potential of As(III) was reduced in the binary system over the entire pH range (Figure 2D), when compared to the single solute system (Figure 1C). Similar results were observed in a recent study [36], which showed the strong inhibitory influence on As(III) adsorption onto ferrihydrite, due to the presence of Sb(III) and Sb(V) species. The removal efficiencies and adsorption sequences of Sb(III) under the influence of As(III) and As(V) were similar for the pH range (5–8) (Figure 2B,D), indicating that both As species had little effect on Sb(III) adsorption. At pH 4, approximately 27% more Sb(III) removal was observed in the presence of As(V) than As(III), thus indicating the inhibitory effect of As(III) on Sb(III) species at low pH (Figure 2B). In addition, at alkaline pH (viz. (9–10)), the Sb(III) removal was significantly inhibited in the Sb(III)/As(V) binary system, due to the dissociation of precipitated Fe under these conditions (Figure 2A,B,D). Elsewhere, the Sb(III) showed stronger adsorption affinity than As(III) using FC over a broad pH range.

Compared to the removal phenomenon of As(III) and Sb(III) in a binary system, the As(V) and Sb(V) showed distinct removal using FC under these conditions. The presence of Sb(III) and Sb(V) species showed similar As(V) removal trend of ~90%–100% from pH (4–7) and decreased upon further increasing pH (Figure 2C). Besides the enhanced Fe solubility under extremely basic conditions (Figure 2A), the more negative effect on As(V) removal was observed in As(V)/Sb(V) binary system (Figure 2C), suggesting the competition of As(V) with Sb(V) on available FC surface sites. However, at pH 8, the strongest adsorption density (18.24 g/mol) for As(V) in As(V)/Sb(III) binary system was observed (Figure 2E). The coexistence of Sb(III) in such binary system had remarkably reduced the Fe solubility (Figure 2A) and the dominant form of Fe(III) and As(V) was $Fe(OH)_2^+$ and $HAsO_4^{2-}$ respectively (Figure S1 and Table S1). The strong electrostatic attraction from negatively charged As(V) towards positively charged Fe(III) hydrolyzed species may have contributed to such strong binding affinity of As(V) under such an environment [14,45]. In comparison with As(V), the removal efficiency and adsorption affinity of Sb(V) in the presence of As(III) and As(V) was different, indicating that the two As species had different effects on Sb(V) removal. Even though almost complete Fe precipitation occurred at pH (4–7) in Sb(V)/As(III) and Sb(V)/As(V) binary systems (Figure 2A), more reduction in Sb(V) removal by FC was observed under the influence of As(V) than As(III) (Figure 2C,E). Similar observations were previously reported [36], which showed the greater inhibitory effect of As(V) on Sb(V), when compared with As(III). However, in the present study, significant reduction in Sb(V) removal (1.75%) in the presence of As(V) was observed at pH 8, which occurred due to the enhanced Fe solubility under these pH conditions (Figure 2A,C). At pH (9 and 10), negligible Sb(V) removal was observed in the Sb(V)/As(V) binary system, while around 9%–12% Sb(V) removal was observed in the Sb(V)/As(III) system (Figure 2C). In general, the adsorption potential of Sb(V) was inhibited to a greater extent in the presence of As(V), as compared to As(III), over a broad pH range. This may be

attributable to the As(V) having a higher charge density and relative smaller spatial structure [16,53]. The steric hindrance of As(V) would be lower than that of Sb(V), which increases the adhesion ability of As(V) on FC precipitates and thus the more active surface sites will be occupied by As(V) [7,54], which easily blocks the dispersion of Sb(V) species on the precipitated Fe surface [55]. Therefore, As(V) species showed stronger adsorption density as compared to Sb(V) in the binary system, as shown in Figure 2E. In summary, the adsorption sequence of As and Sb species by FC in binary system at pH (5, 7 and 9) can be arranged in the orders of (As(V) > Sb(III) > Sb(V) > As(III)), (As(V) > Sb(III) > Sb(V) > As(III)) and (Sb(III) > As(V) ≈ As(III) > Sb(V)), respectively.

3.1.3. Quaternary System

Figure 3A shows the Fe solubility and competitive removal of total As, as well as total Sb species, under a quaternary system, using FC coagulation across various pH range. Interestingly, the co-presence of redox species (As(III), Sb(III), As(V) and Sb(V)) significantly reduced the Fe solubility, irrespective of pH (Figure 3A). Under acidic conditions, the coexistence of negatively charged As(V) and Sb(V) might be responsible for such a phenomenon, as discussed in Section 3.1.2. However, at alkaline conditions, the neutral As(III) and Sb(III) species must have actively interacted with As(V)/Sb(V) induced Fe(III) dissociated hydroxyl species, which resulted in the formation of a substantial amount of FC precipitates [15]. Moreover, the change in pH was also monitored before and after coagulation in the quaternary system, which showed that pH remains consistent, hence did not show any effect on FC precipitation under those conditions (Table S4 of the SI).

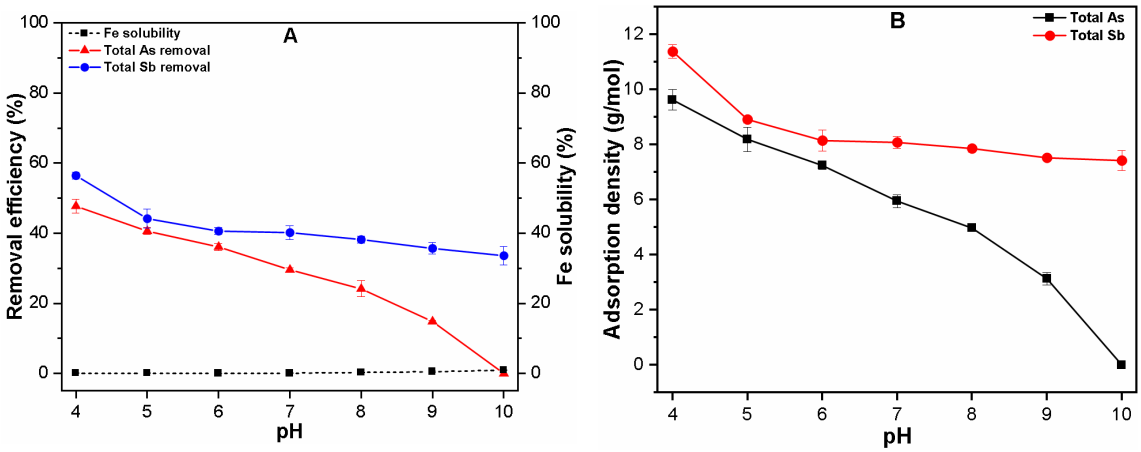

Figure 3. The quaternary system of As and Sb species showing (**A**) Fe solubility (%) and removal efficiency (%); (**B**) Adsorption densities (g/mol) under various pH range (4–10) with 0.1 mM FC coagulant dose.

Figure 3A shows the competitive removal of Total As and Sb under quaternary system over a broad pH range. As shown, the total Sb removal was found to be higher than the total As regardless of pH; moreover, under acidic conditions, the highest As (47.74%) and Sb (56.46%) removal were achieved, which continuously decreased upon increasing pH. At neutral pH, around 40.2% Sb and 29.59% As removal were observed. In contrast at extremely basic condition (viz. pH 10), about 33.61% Sb removal was achieved with negligible As removal. Similarly, the adsorption affinity of total Sb was higher than total As over the entire pH range (Figure 3B). Under basic conditions, the difference between adsorbed Sb and adsorbed As increased to a large extent, indicating much superior Sb affinity towards FC precipitates than As in such an environment.

Based on observations in a binary system, the relatively similar adsorption affinity of As and Sb around pH (4–5) under quaternary conditions may be ascribed to As(V) being preferentially removed at such pH range, with strong inhibitory effect on As(III) sorption. Moreover, a recent study [56] reported the reduction in total As removal in the As(III)/As(V) binary system. Our previous study [13]

also indicated the reduction in total Sb removal in mixed Sb(III)-Sb(V) aqueous solution but relatively less reduction in total Sb removal was observed, compared to total As removal [13,56]. The strongest adsorption affinity of Sb(III) has also been previously reported in the quaternary system [36]. Therefore, based on the previous literature and current observations, it can be inferred that Sb(III) contains a high adsorption affinity, followed by As(V), under such pH (6–7) range. Similarly, under basic pH (8–10), the adsorption affinity of Sb becomes superior in the quaternary system, due to the adhesion ability of As(V) and Sb(V) being affected by strong electrostatic repulsion forces between molecules and FC species in such aqueous media [45]. Also, the antagonistic effect on As(III) sorption towards FC surface sites was also observed in the presence of both Sb species (Figure 2D). Based on the binary and quaternary system trends, the adsorption envelops of As and Sb species under quaternary conditions at pH (5, 7 and 9) can be anticipated in the order of (As(V) > Sb(III) > Sb(V) > As(III)), (Sb(III) > As(V) > Sb(V) > As(III)) and (Sb(III) > As(III) > As(V) ≈ Sb(V)), respectively.

3.2. Modeling As and Sb Coagulation Data by Isotherm Studies

3.2.1. Single Solute System

Figure 4 illustrates the adsorption isotherms of As(III, V) and Sb(III, V) on FC precipitates in the single solute system. The adsorption data were fitted with Langmuir and Freundlich (Figure 4A,B) models, while Table 1 shows the fitted parameters. These show that the Sb(III) species revealed the strongest adsorption affinity onto FC surface sites with the regression (R^2) values of 0.985 (Langmuir) and 0.990 (Freundlich), respectively. The R^2 value for As(III) species was determined to be (0.917 and 0.984) for the Langmuir and Freundlich adsorption models, respectively, thus suggesting the multilayer formation of As(III) species on FC precipitates. In contrast, the Langmuir model (R^2:0.994) fitted better than the Freundlich model (R^2:0.852) for Sb(V) species, which indicates the monolayer formation of Sb(V) species onto FC precipitates [57]. Unlike other contaminants, the adsorption isotherm fitting parameters for As(V) species were not obtained using both models. This contradicted the findings of previous studies [1,36], which reported Freundlich fitting for As(V) species on ferrihydrite surface. The possible reason might be related to the adsorbent dosage and initial concentration of As(V) in the aqueous solution. The result of the present adsorption study indicates the decrease in the adsorption capacity at initial As(V) concentration greater than 2 mg/L with 0.1 mM FC dose. In order to further clarify such distinct adsorption behavior of As(V), FC precipitates were monitored during whole adsorption experiments. The results revealed that the Fe solubility was significantly enhanced when the initial concentration of As(V) rose above 2 mg/L (Figure S2 of the SI). This phenomenon might be attributed to at pH 7, the negatively charged As(V) species ($HAsO_4^{2-}$) being strongly bound onto the surface of positively charged Fe(III) hydrolyzed species ($Fe(OH)_2^{+}$) [14]. When the concentration of $HAsO_4^{2-}$ increases from (0 to 1.5) mg/L, charge neutralization occurs; while on further increasing the concentration of $HAsO_4^{2-}$ above 2 mg/L, charge reversal of the Fe(III)-complex occurs, thus weakening the Fe–O bond and lowering the energy barrier [51]. As a result, dissolution of FC precipitates was proceeded to pertain to further increase in the concentration of As(V) species in such aqueous media.

Table 1. Adsorption isotherm parameters of As(III) and Sb(III, V) on FC precipitates in the single solute system.

Contaminants	Langmuir Fitting			Freundlich Fitting		
	K_L (L/mg)	q_m (g/mol)	R^2	K_F (g/mol) (L/mg) $^{\frac{1}{n}}$	n	R^2
As(III)	0.559	38.01	0.917	13.346	2.221	0.984
Sb(III)	0.622	111.95	0.985	38.359	1.586	0.990
Sb(V)	3.961	32.74	0.994	20.255	3.457	0.852

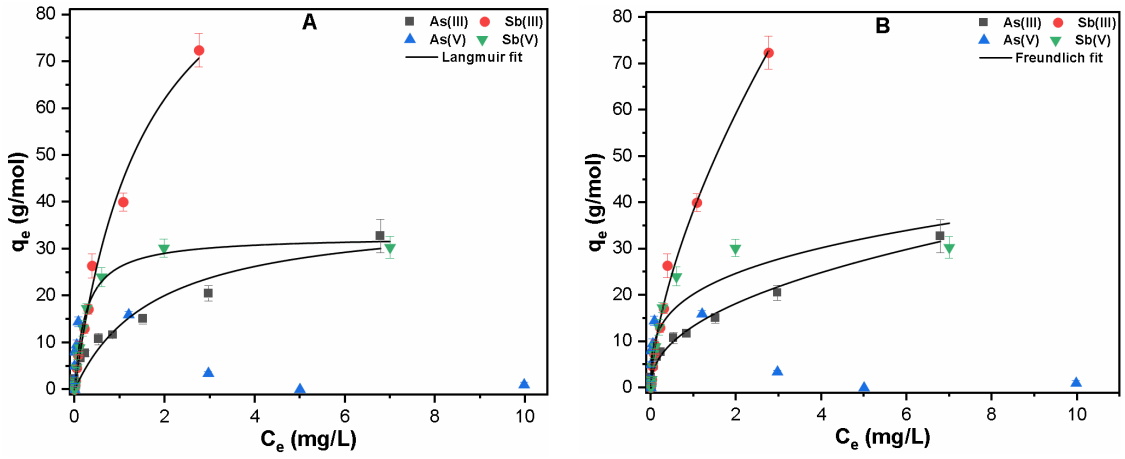

Figure 4. Under the initial As and Sb concentrations of (0.1 to 10) mg/L, pH: 7 and 0.1 mM FC dose, showing (**A**) Langmuir; and (**B**) Freundlich fitting of the As and Sb coagulation data for the single solute system.

3.2.2. Binary System

Figure 5 shows the experimental results of the binary system containing As and Sb species and the Langmuir and Freundlich model fits under various initial concentrations at pH 7. In the binary system, Sb(III) species showed a significant increase in adsorption capacity onto FC precipitates in the presence of As(III) and As(V) species. These results are consistent with the previous findings that indicated that the Sb(III) species did not reach the isotherm plateau [36]. The adsorption capacity of As(III) species showed inhibitory effect on As(III) sorption with increasing concentration in the presence of Sb(III) and Sb(V) species (Figure 5A,C). In contrast to the single solute system, the As(V) species shows an increase in adsorption potential with increasing concentration in the binary system (Figure 5B,D). Figure S3 of the SI shows that the significant decrease in Fe solubility in the binary system might result in such an increase in As(V) adsorption capacity. Moreover, the Sb(V) adsorption onto FC precipitates was significantly affected in a binary system, as compared to any other species (Figure 5B,D). The Freundlich model was preferred for the adsorption of As(V) and Sb(V) in the binary systems, as indicated by their strong correlation coefficient (Table 2). However, the As(III) and Sb(III) species showed distinct adsorption phenomena, depending upon the type of species present in the system. For example, the As(III) species followed the Langmuir model in the As(III)/Sb(V) binary system and the Freundlich model in the As(III)/Sb(III) binary system. In general, such behavior is in good agreement with the observed competition between the species and available FC surface sites in the binary system.

Table 2. Adsorption isotherm parameters of As and Sb species on FC precipitates in the binary system.

Sample	Solutes	Langmuir Fitting			Freundlich Fitting		
		K_L (L/mg)	q_m (g/mol)	R^2	K_F (g/mol) (L/mg) $\frac{1}{n}$	n	R^2
As(III)/Sb(III)	As(III)	0.355	23.11	0.981	6.169	1.984	0.987
	Sb(III)	0.400	132.29	0.962	34.666	1.465	0.950
As(III)/Sb(V)	As(III)	0.264	40.99	0.908	8.308	1.661	0.861
	Sb(V)	0.586	12.84	0.550	4.896	2.608	0.652
As(V)/Sb(III)	As(V)	1.053	53.32	0.848	21.258	2.276	0.895
	Sb(III)	0.00001	5771510	0.962	42.400	0.729	0.996
As(V)/Sb(V)	As(V)	0.135	116.97	0.945	15.574	1.497	0.951
	Sb(V)	0.122	49.19	0.928	7.028	1.696	0.967

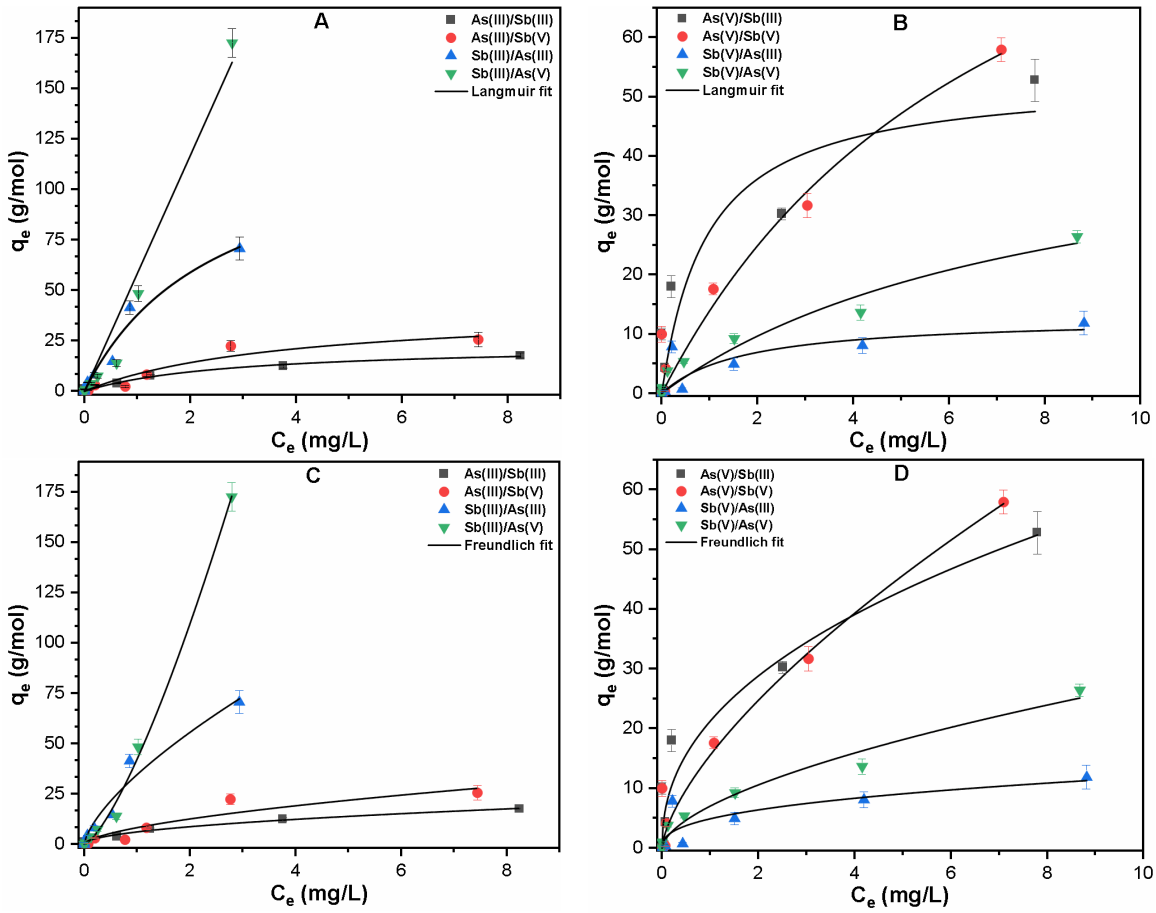

Figure 5. Under initial As and Sb concentrations of (0.1 to 10) mg/L, pH: 7 and 0.1 mM FC dose, showing (**A**,**B**) Langmuir; and (**C**,**D**) Freundlich fitting of the As and Sb coagulation data for the binary system.

3.2.3. Quaternary System

Figure 6 shows the competitive adsorption experimental results of the quaternary system and their non-linear isotherm fittings. The results indicate that the adsorption affinity of Sb species rivals the adsorption capacity of As species on FC precipitates in coexisting environments at neutral pH (Figure 6A,B). Similar to the binary system, the total Sb adsorption onto the sites of FC surface becomes highly favorable in the presence of As species. Besides complete FC precipitation (Figure S4 of the SI), such an adsorption phenomenon indicates that only Sb species would preferentially adsorb onto FC precipitates in a complex heterogeneous environment containing a higher concentration of both species. Furthermore, Table 3 shows the Langmuir and Freundlich fitting parameters for the total Sb species (i.e., Sb(III, V)), which further confirms the strong Sb adsorption affinity of 82.04 g/mol under the quaternary system.

Table 3. Parameters of the Langmuir and Freundlich adsorption models for Sb species on FC precipitates in the quaternary system.

Solutes	Langmuir Fitting			Freundlich Fitting		
	K_L (L/mg)	q_m (g/mol)	R^2	K_F (g/mol) (L/mg) $\frac{1}{n}$	n	R^2
Sb(III, V)	0.069	82.04	0.995	6.82	1.485	0.998

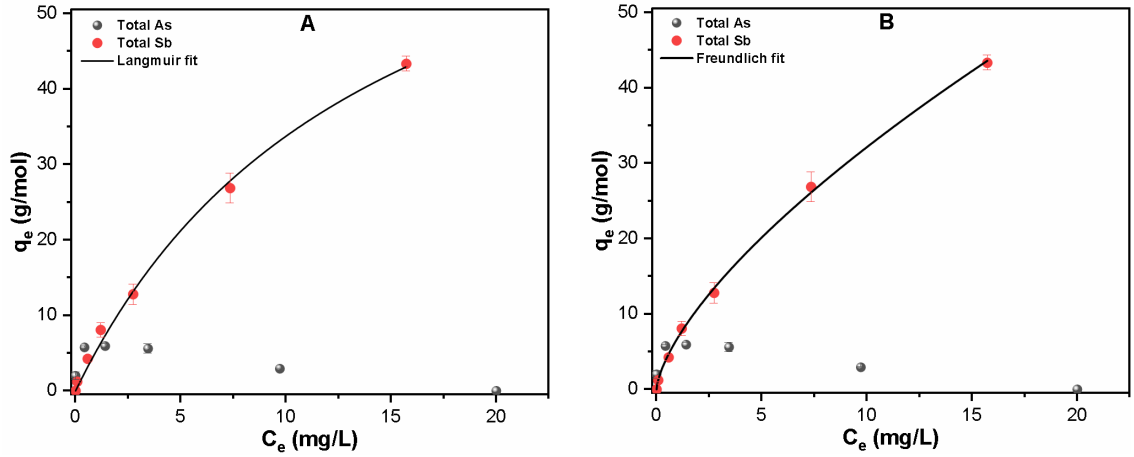

Figure 6. Under the initial As and Sb concentrations of (0.1 to 10) mg/L, pH: 7 and 0.1 mM FC dose, showing the (**A**) Langmuir; and (**B**) Freundlich fitting of the As and Sb coagulation data for the quaternary system.

3.3. Mechanism of As and Sb Removal by FC Coagulation

The FT-IR analysis of FC precipitates in single, binary and quaternary systems was recorded to explore the bond formation and possible removal mechanism, as shown in Figure 7. The broad peak in all flocs around 3384–3396 cm^{-1} was ascribed to the polar interaction of Fe ions and their hydrolyzed products, which tends to form complexes with contaminants [58]. The peaks appearing at (~1632 and 900–1367) cm^{-1} were ascribed to the deformation of water molecules and enrichment of aliphatic/carbohydrates OH functional groups, respectively [59,60]. In comparison with the pristine spectra of all species (Figure S5), except As(V), no significant shift in other FC flocs was observed in the single solute system (Figure 7A). The shift in the peak of As(V) from 832–812 cm^{-1} further clarified the strong adsorption potential of As(V) via complexation in the single solute system [59]. The flocs spectra in the binary systems of Sb(III)/As(III) and Sb(V)/As(III) indicated a negligible shift in their peaks, when compared with pristine contaminants. However, the significant shift in As(V) peak from (832 to (802–810)) cm^{-1} was observed in their binary system, which indicates that the presence of Sb species will rarely have a competitive effect. Interestingly, after reaction with FC flocs, the binary system of Sb(V)/As(V) showed the new peak at (694 instead of 682) cm^{-1}, which may be attributable to the Sb(III)-O vibration.

In the quaternary system, the strong stretching vibration of Sb(III)-O were also observed in the range (~455–462) cm^{-1} in all flocs under all pH conditions. In the case of pH (5 and 7), the peaks appearing at (455, 596 and around (802–818)) cm^{-1} correspond to Sb(III)-O, Sb(V)-O and As(V)-O stretching vibrations, which further clarifies that these groups could be involved in complex coordination with FC precipitates during their competitive adsorption [57,59].

At pH 9, the peak at 586 cm^{-1} appears with higher intensity, due to the interaction between As(III) species and FC flocs under competitive environment [39]. Furthermore, the intensity of the peak at 810 cm^{-1} is significantly reduced, which indicates the inhibition of As(V) adsorption onto FC flocs under basic pH conditions. Thus, the significant shifts, as well as distinct intensity peaks in the contaminant FC flocs, well support the adsorption sequence of redox species. Similar to As, the most plausible chemical interactions between Sb and FC precipitates were the formation of inner-sphere complexes with OH functional groups at the surface of the FC hydrolyzed products [30,61]. Therefore, it can be inferred from the adsorption capacities and FT-IR spectra that the possible removal mechanism for As and Sb species might be the combination of charge neutralization and inner sphere complexation. This mechanism is consistent with previous research [7,8,36,52], working on the removal of heavy metals by coagulation.

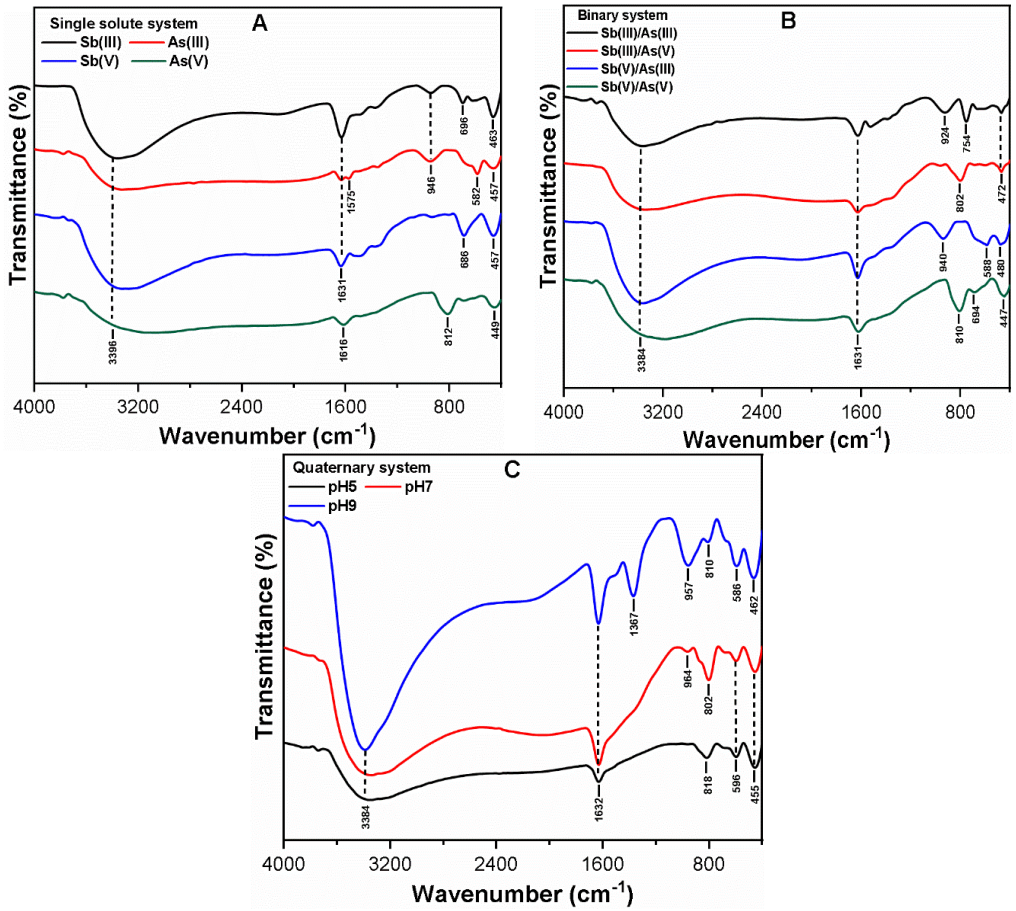

Figure 7. FT-IR spectra analysis of FC contaminants flocs showing (**A**) Single solute; (**B**) binary; and (**C**) quaternary system, after coagulation with 0.1 mM FC dose.

4. Conclusions

In this study, we systematically investigated the influence of pH and contaminant loading of four redox species on Fe solubility, as well as their adsorptive removal behavior, in the single, binary and quaternary system. The results of the single solute system showed the adverse effect on Fe solubility in the presence of pentavalent species at the elevated pH, thereby reducing the overall adsorption capacity of As(V) and Sb(V). Moreover, the adsorption density of both species in the binary system is significantly affected by the increase in Fe solubility under extremely alkaline condition. The competitive adsorption behavior in the presence of the four redox species differs remarkably at different pH conditions. The association of all species has a synergistic effect on total Sb removal, while having a strong inhibitory effect on As removal. The decrease in adsorption capacity of As(V) in the single system at higher contaminant loading was observed, while in the binary system, Sb(III) showed a strong adsorption potential in comparison to other species. Moreover, in the quaternary system, the higher adsorption capacity of Sb indicates the synergistic effect in the co-presence of other species. The FT-IR analysis of FC contaminant flocs reveals that mechanisms, such as charge neutralization and inner sphere complexation, might be involved in the removal of all species by coagulation. These outcomes advance understanding of the removal efficiency and removal mechanism of these toxic contaminants, as well as the optimization of coagulant thereafter.

Supplementary Materials: The following are available online at http://www.mdpi.com/2075-163X/8/12/574/s1, Table S1: Major speciation of trivalent (As(III) and Sb(III)) and pentavalent (As(V) and Sb(V)) species at various pH conditions obtained using Visual MINTEQ. Table S2: Single solute system showing change in pH after ferric chloride (FC) coagulation in the absence and presence of As and Sb species. Table S3: Binary system showing change in pH after FC coagulation in the presence of As and Sb species in binary mode. Table S4: Quaternary

system showing change in pH after FC coagulation in the presence of As and Sb species in multicomponent environment. Figure S1: Speciation of Fe(III) species derived from Visual MINTEQ. Figure S2: Single solute system of As and Sb showing Fe solubility behavior at pH 7, 0.1 mM FC dose and varying initial concentration of (0–10) mg/L. Figure S3: Binary system of As and Sb showing Fe solubility behavior at pH 7, 0.1 mM FC dose and varying initial As-Sb concentration of (0–10) mg/L of each species, respectively. Figure S4: Quaternary system of As and Sb showing Fe solubility behavior at pH 7, 0.1 mM FC dose and varying initial As-Sb concentration of (0–10) mg/L of each species, respectively. Figure S5: FT-IR Spectra of pristine (A) FC, (B) and (C) Sb(III,V) and (B) and (C) As(III,V) Species.

Author Contributions: M.A.I. and I.T.Y. designed the study; M.A.I. and R.K. performed the experiment and analyzed the data; D.R.P., B.A.A. and A.U. provided critical feedback and helped shape the research; M.A.I. wrote the final version of the manuscript.

Funding: This research received no external funding.

Conflicts of Interest: The authors declare no conflict of interest.

References

1. Wu, D.; Sun, S.-P.; He, M.; Wu, Z.; Xiao, J.; Chen, X.D.; Wu, W.D. As (V) and Sb (V) co-adsorption onto ferrihydrite: Synergistic effect of Sb (V) on As (V) under competitive conditions. *Environ. Sci. Pollut. Res.* **2018**, *25*, 14585–14594. [CrossRef] [PubMed]
2. Mubarak, H.; Chai, L.-Y.; Mirza, N.; Yang, Z.-H.; Pervez, A.; Tariq, M.; Shaheen, S.; Mahmood, Q. Antimony (Sb)–pollution and removal techniques–critical assessment of technologies. *Toxicol. Environ. Chem.* **2015**, *97*, 1296–1318. [CrossRef]
3. Filella, M.; Belzile, N.; Chen, Y.-W. Antimony in the environment: A review focused on natural waters: I. Occurrence. *Earth-Sci. Rev.* **2002**, *57*, 125–176. [CrossRef]
4. U.S.G.S. *Mineral Commodity Summaries 2017: US Geological Survey*; USGS: Reston, VA, USA, 2017.
5. Hansell, C. All manner of antimony. *Nat. Chem.* **2015**, *7*, 88. [CrossRef] [PubMed]
6. Rahman, M.M.; Saha, K.C.; Mukherjee, S.C.; Pati, S.; Dutta, R.N.; Roy, S.; Quamruzzaman, Q.; Rahman, M.; Chakraborti, D. Groundwater arsenic contamination in Bengal delta and its health effects. In *Safe and Sustainable Use of Arsenic-Contaminated Aquifers in the Gangetic Plain*; Springer: Berlin, Germany, 2015; pp. 215–253.
7. Wang, H.; Tsang, Y.F.; Wang, Y.; Sun, Y.; Zhang, D.; Pan, X. Adsorption capacities of poorly crystalline Fe minerals for antimonate and arsenate removal from water: Adsorption properties and effects of environmental and chemical conditions. *Clean Technol. Environ. Policy* **2018**, *20*, 2169–2179. [CrossRef]
8. Fu, Z.; Wu, F.; Mo, C.; Deng, Q.; Meng, W.; Giesy, J.P. Comparison of arsenic and antimony biogeochemical behavior in water, soil and tailings from Xikuangshan, China. *Sci. Total Environ.* **2016**, *539*, 97–104. [CrossRef] [PubMed]
9. Hiller, E.; Lalinská, B.; Chovan, M.; Jurkovič, Ľ.; Klimko, T.; Jankulár, M.; Hovorič, R.; Šottník, P.; Fľaková, R.; Ženišová, Z. Arsenic and antimony contamination of waters, stream sediments and soils in the vicinity of abandoned antimony mines in the Western Carpathians, Slovakia. *Appl. Geochem.* **2012**, *27*, 598–614. [CrossRef]
10. Wang, X.; He, M.; Xi, J.; Lu, X. Antimony distribution and mobility in rivers around the world's largest antimony mine of Xikuangshan, Hunan Province, China. *Microchem. J.* **2011**, *97*, 4–11. [CrossRef]
11. He, M. Distribution and phytoavailability of antimony at an antimony mining and smelting area, Hunan, China. *Environ. Geochem. Health* **2007**, *29*, 209–219. [CrossRef] [PubMed]
12. Cai, J.; Salmon, K.; DuBow, M.S. A chromosomal ars operon homologue of Pseudomonas aeruginosa confers increased resistance to arsenic and antimony in *Escherichia coli*. *Microbiology* **1998**, *144*, 2705–2729. [CrossRef]
13. Inam, M.A.; Khan, R.; Park, D.R.; Lee, Y.-W.; Yeom, I.T. Removal of Sb (III) and Sb (V) by Ferric Chloride Coagulation: Implications of Fe Solubility. *Water* **2018**, *10*, 418. [CrossRef]
14. Wang, Y.; Duan, J.; Liu, S.; Li, W.; van Leeuwen, J.; Mulcahy, D. Removal of As (III) and As (V) by ferric salts coagulation–Implications of particle size and zeta potential of precipitates. *Sep. Purif. Technol.* **2014**, *135*, 64–71. [CrossRef]
15. Leuz, A.-K.; Mönch, H.; Johnson, C.A. Sorption of Sb (III) and Sb (V) to goethite: Influence on Sb (III) oxidation and mobilization. *Environ. Sci. Technol.* **2006**, *40*, 7277–7282. [CrossRef] [PubMed]
16. Wilson, S.C.; Lockwood, P.V.; Ashley, P.M.; Tighe, M. The chemistry and behaviour of antimony in the soil environment with comparisons to arsenic: A critical review. *Environ. Pollut.* **2010**, *158*, 1169–1181. [CrossRef] [PubMed]

17. Ungureanu, G.; Santos, S.; Boaventura, R.; Botelho, C. Arsenic and antimony in water and wastewater: Overview of removal techniques with special reference to latest advances in adsorption. *J. Environ. Manag.* **2015**, *151*, 326–342. [CrossRef] [PubMed]
18. Smith, A.H.; Hopenhayn-Rich, C.; Bates, M.N.; Goeden, H.M.; Hertz-Picciotto, I.; Duggan, H.M.; Wood, R.; Kosnett, M.J.; Smith, M.T. Cancer risks from arsenic in drinking water. *Environ. Health Perspect.* **1992**, *97*, 259–267. [CrossRef] [PubMed]
19. Herath, I.; Vithanage, M.; Bundschuh, J. Antimony as a global dilemma: Geochemistry, mobility, fate and transport Title. *Environ. Pollut.* **2017**, *223*, 545–559. [CrossRef]
20. MOE. MOE Korea. 2015. Available online: http://www.me.go.kr/home/web/index.do?menuId=68 (accessed on 7 August 2018).
21. Antelo, J.; Avena, M.; Fiol, S.; López, R.; Arce, F. Effects of pH and ionic strength on the adsorption of phosphate and arsenate at the goethite–water interface. *J. Colloid Interface Sci.* **2005**, *285*, 476–486. [CrossRef]
22. Okkenhaug, G.; Zhu, Y.-G.; He, J.; Li, X.; Luo, L.; Mulder, J. Antimony (Sb) and arsenic (As) in Sb mining impacted paddy soil from Xikuangshan, China: Differences in mechanisms controlling soil sequestration and uptake in rice. *Environ. Sci. Technol.* **2012**, *46*, 3155–3162. [CrossRef]
23. Cornell, R.M.; Schwertmann, U. *The Iron Oxides: Structure, Properties, Reactions, Occurrence and Uses*; John Wiley & Sons: Hoboken, NJ, USA, 2003; pp. 167–168.
24. Pedersen, H.D.; Postma, D.J.; Jakobsen, R.; Larsen, O. *The Transformation of Fe (III) Oxides Catalysed by* Fe^{2+} *and the Fate of Arsenate during Transformation and Reduction of Fe (III) Oxides*; DTU Environment: Lyngby, Denmark, 2006; ISBN 8791855020.
25. Biber, M.V.; dos Santos Afonso, M.; Stumm, W. The coordination chemistry of weathering: IV. Inhibition of the dissolution of oxide minerals. *Geochim. Cosmochim. Acta* **1994**, *58*, 1999–2010. [CrossRef]
26. Ponnamperuma, F.N. The chemistry of submerged soils. In *Advances in Agronomy*; Elsevier: Berlin, Germany, 1972; Volume 24, pp. 29–96. ISBN 0065-2113.
27. Waite, T.D.; Morel, F.M.M. Photoreductive dissolution of colloidal iron oxides in natural waters. *Environ. Sci. Technol.* **1984**, *18*, 860–868. [CrossRef] [PubMed]
28. LeMonte, J.J.; Stuckey, J.W.; Sanchez, J.Z.; Tappero, R.; Rinklebe, J.; Sparks, D.L. Sea level rise induced arsenic release from historically contaminated coastal soils. *Environ. Sci. Technol.* **2017**, *51*, 5913–5922. [CrossRef] [PubMed]
29. Frohne, T.; Rinklebe, J.; Diaz-Bone, R.A.; Du Laing, G. Controlled variation of redox conditions in a floodplain soil: Impact on metal mobilization and biomethylation of arsenic and antimony. *Geoderma* **2011**, *160*, 414–424. [CrossRef]
30. Shan, C.; Ma, Z.; Tong, M. Efficient removal of trace antimony (III) through adsorption by hematite modified magnetic nanoparticles. *J. Hazard. Mater.* **2014**, *268*, 229–236. [CrossRef] [PubMed]
31. Navarro, P.; Alguacil, F.J. Adsorption of antimony and arsenic from a copper electrorefining solution onto activated carbon. *Hydrometallurgy* **2002**, *66*, 101–105. [CrossRef]
32. Bao, C.; Xie, Y.; Liu, Y.; Srivastava, A. Reverse Engineering-Based Hardware Trojan Detection. In *The Hardware Trojan War*; Springer: Berlin, Germany, 2018; pp. 269–288.
33. Guo, X.; Wu, Z.; He, M. Removal of antimony (V) and antimony (III) from drinking water by coagulation–flocculation–sedimentation (CFS). *Water Res.* **2009**, *43*, 4327–4335. [CrossRef] [PubMed]
34. Guo, X.; Wu, Z.; He, M.; Meng, X.; Jin, X.; Qiu, N.; Zhang, J. Adsorption of antimony onto iron oxyhydroxides: Adsorption behavior and surface structure. *J. Hazard. Mater.* **2014**, *276*, 339–345. [CrossRef]
35. Qi, P.; Pichler, T. Sequential and simultaneous adsorption of Sb (III) and Sb (V) on ferrihydrite: Implications for oxidation and competition. *Chemosphere* **2016**, *145*, 55–60. [CrossRef]
36. Qi, P.; Pichler, T. Competitive adsorption of As (III), As (V), Sb (III) and Sb (V) onto ferrihydrite in multi-component systems: Implications for mobility and distribution. *J. Hazard. Mater.* **2017**, *330*, 142–148. [CrossRef]
37. Lan, B.; Wang, Y.; Wang, X.; Zhou, X.; Kang, Y.; Li, L. Aqueous arsenic (As) and antimony (Sb) removal by potassium ferrate. *Chem. Eng. J.* **2016**, *292*, 389–397. [CrossRef]
38. Kang, M.; Kamei, T.; Magara, Y. Comparing polyaluminum chloride and ferric chloride for antimony removal. *Water Res.* **2003**, *37*, 4171–4179. [CrossRef]
39. Guo, W.; Fu, Z.; Wang, H.; Liu, S.; Wu, F.; Giesy, J.P. Removal of antimonate (Sb (V)) and antimonite (Sb (III)) from aqueous solutions by coagulation-flocculation-sedimentation (CFS): Dependence on influencing factors and insights into removal mechanisms. *Sci. Total Environ.* **2018**, *644*, 1277–1285. [CrossRef]

40. Qiao, J.; Jiang, Z.; Sun, B.; Sun, Y.; Wang, Q.; Guan, X. Arsenate and arsenite removal by $FeCl_3$: Effects of pH, As/Fe ratio, initial As concentration and co-existing solutes. *Sep. Purif. Technol.* **2012**, *92*, 106–114. [CrossRef]
41. Hering, J.G.; Chen, P.; Wilkie, J.A.; Elimelech, M.; Liang, S. Arsenic removal by ferric chloride. *J. Am. Water Work. Assoc.* **1996**, *88*, 155–167. [CrossRef]
42. Hering, J.G.; Chen, P.-Y.; Wilkie, J.A.; Elimelech, M. Arsenic removal from drinking water during coagulation. *J. Environ. Eng.* **1997**, *123*, 800–807. [CrossRef]
43. Langmuir, I. The adsorption of gases on plane surfaces of glass, mica and platinum. *J. Am. Chem. Soc.* **1918**, *40*, 1361–1403. [CrossRef]
44. Freundlich, H.M.F. Uber Die Adsorption in Losungen. *Z. Phys. Chem. (Leipz.)* **1906**, *57*, 385–470. (In German) [CrossRef]
45. Yan, D.; Li, H.-J.; Cai, H.-Q.; Wang, M.; Wang, C.-C.; Yi, H.-B.; Min, X.-B. Microscopic insight into precipitation and adsorption of As (V) species by Fe-based materials in aqueous phase. *Chemosphere* **2018**, *194*, 117–124. [CrossRef] [PubMed]
46. Zinder, B.; Furrer, G.; Stumm, W. The coordination chemistry of weathering: II. Dissolution of Fe(III) oxides. *Geochim. Cosmochim. Acta* **1986**, *50*, 1861–1869. [CrossRef]
47. Stumm, W. Reactivity at the mineral-water interface: Dissolution and inhibition. *Colloids Surf. A Physicochem. Eng. Asp.* **1997**, *120*, 143–166. [CrossRef]
48. Stone, A.T.; Torrents, A.; Smolen, J.; Vasudevan, D.; Hadley, J. Adsorption of organic compounds possessing ligand donor groups at the oxide/water interface. *Environ. Sci. Technol.* **1993**, *27*, 895–909. [CrossRef]
49. Stone, A.T. Reactions of extracellular organic ligands with dissolved metal ions and mineral surfaces. *Rev. Mineral. Geochem.* **1997**, *35*, 309–344.
50. Ohshima, H. DLVO Theory of Colloid Stability. In *Electrical Phenomena at Interfaces*, 2nd ed.; Routledge: Abingdon, UK, 2018; pp. 119–136.
51. Stumm, W. The Inner-Sphere Surface Complex. *Adv. Chem.* **1995**, *244*, 1–32.
52. Han, Y.-S.; Seong, H.J.; Chon, C.-M.; Park, J.H.; Nam, I.-H.; Yoo, K.; Ahn, J.S. Interaction of Sb (III) with iron sulfide under anoxic conditions: Similarities and differences compared to As (III) interactions. *Chemosphere* **2018**, *195*, 762–770. [CrossRef] [PubMed]
53. Pauling, L. The formulas of antimonic acid and the antimonates. *J. Am. Chem. Soc.* **1933**, *55*, 1895–1900. [CrossRef]
54. Wang, H.; Wang, Y.; Sun, Y.; Pan, X.; Zhang, D.; Tsang, Y.F. Differences in Sb (V) and As (V) adsorption onto a poorly crystalline phyllomanganate (δ-MnO_2): Adsorption kinetics, isotherms, and mechanisms. *Process Saf. Environ. Prot.* **2018**, *113*, 40–47. [CrossRef]
55. Deng, S.; Yu, Q.; Huang, J.; Yu, G. Removal of perfluorooctane sulfonate from wastewater by anion exchange resins: Effects of resin properties and solution chemistry. *Water Res.* **2010**, *44*, 5188–5195. [CrossRef]
56. Hou, J.; Luo, J.; Song, S.; Li, Y.; Li, Q. The remarkable effect of the coexisting arsenite and arsenate species ratios on arsenic removal by manganese oxide. *Chem. Eng. J.* **2017**, *315*, 159–166. [CrossRef]
57. Xu, W.; Wang, H.; Liu, R.; Zhao, X.; Qu, J. The mechanism of antimony (III) removal and its reactions on the surfaces of Fe–Mn binary oxide. *J. Colloid Interface Sci.* **2011**, *363*, 320–326. [CrossRef]
58. Khan, R.; Inam, M.; Park, D.; Zam Zam, S.; Shin, S.; Khan, S.; Akram, M.; Yeom, I. Influence of Organic Ligands on the Colloidal Stability and Removal of ZnO Nanoparticles from Synthetic Waters by Coagulation. *Processes* **2018**, *6*, 170. [CrossRef]
59. Zhang, G.-S.; Qu, J.-H.; Liu, H.-J.; Liu, R.-P.; Li, G.-T. Removal mechanism of As (III) by a novel Fe–Mn binary oxide adsorbent: Oxidation and sorption. *Environ. Sci. Technol.* **2007**, *41*, 4613–4619. [CrossRef] [PubMed]
60. Khan, R.; Inam, M.A.; Zam, S.Z.; Park, D.R.; Yeom, I.T. Assessment of Key Environmental Factors Influencing the Sedimentation and Aggregation Behavior of Zinc Oxide Nanoparticles in Aquatic Environment. *Water* **2018**, *10*, 660. [CrossRef]
61. Mitsunobu, S.; Muramatsu, C.; Watanabe, K.; Sakata, M. Behavior of antimony (V) during the transformation of ferrihydrite and its environmental implications. *Environ. Sci. Technol.* **2013**, *47*, 9660–9667. [CrossRef] [PubMed]